The Role of Charge Localization in Current-Driven Dynamics

RYAN JORN,[a] ESTER LIVSHITS,[b] ROI BAER,[b] AND TAMAR SEIDEMAN[a,*]
[a]Department of Chemistry, Northwestern University, Evanston, Ilinois 60208, USA
[b]Institute of Chemistry and The Fritz Haber Center for Molecular Dynamics, The Hebrew University of Jerusalem, Jerusalem 91904, Israel

(Received 15 December 2006)

Abstract. We explore the role of charge localization in current-triggered, resonance-mediated, dynamical events in molecular junctions. To that end we use a simple model for a molecular rattle, a $Li^{+}C_9H_9^{-}$ zwitterion attached between two metal clusters. By varying the size of the metal clusters we systematically vary the degree of delocalization of the electronic orbitals underlying the resonant current, and thus can draw general conclusions regarding the effect of delocalization on dynamical processes induced by resonance inelastic current in molecular electronics.

In the small cluster limit, we find interesting quantum dynamics in the nuclear subspace, corresponding to coherent tunneling of the wave packet through the barrier of an asymmetric double-well potential. These dynamics are rapidly damped with increasing charge delocalization in extended systems.

INTRODUCTION

The fundamental and technological implications of synthesizing electronic devices at the molecular scale have been inspiring progress in molecular electronics for over a decade. Armed with great ambitions and ingenuity, researchers have made advances towards fabricating few- to single-molecule junctions using a variety of means such as electromigration techniques,[1–4] break junction methods,[5–8] and scanning probe microscopies.[9–14] Theoretical progress has been equally intense, with efforts to understand the basic parameters that dictate molecular conductivity, including the terminal group tethering the molecule to the electrode,[15–17] the electronic structure of the molecular backbone,[18,19] and the nature of the bond between the molecule and the electrode surface.[20–25]

While these efforts have focused on understanding the static conductivity of the molecular moiety, the importance of current-driven dynamical events has also been recently demonstrated.[1,26–31] Coupling between the electronic states of the molecule and the continua of states present in the electrodes results in the formation of electronic resonances characterized by a finite lifetime and an energy shift. Provided that these resonance states are energetically close to the Fermi level, they can provide a pathway for current transmission at low bias voltages and contribute to inelastic transport. The possibility of resonant tunneling current inducing large amplitude molecular dynamics, spanning the range from vibrational excitation to bond breaking and chemical reaction, has recently been elucidated in several experimental[27,30,32–36] and theoretical[37–46] studies. In particular, refs 37–39 illustrate the concept of current-driven molecular machines through the examples of a nano-oscillator [37,38] and a unidirectional molecular rotor,[39] whereas refs 32 and 33 demonstrate current-driven single-molecule surface chemistry in the STM-environment.

The inelasticity of resonance-mediated transport is governed by the lifetime of the resonance state as well as the deviation of the resonance state potential energy surface from the neutral surface morphology. In the context of molecular electronics, molecule-derived resonances typically correspond to anionic (electron conduction) or cationic (hole conduction) states, and therefore the resonance transport event is described in terms of charge trapping around the molecule. The temporary presence of an additional charge modifies the

*Author to whom correspondence should be addressed.
E-mail: seideman@chem.northwestern.edu

potential energy surface experienced by the nuclei, and the molecule finds itself in an excited configuration on the charged surface. As a result, the nuclear subsystem evolves in time on the resonance surface while continuously decaying to the neutral state, subject to the finite lifetime of the electronic resonance. Qualitatively, the probability of molecular excitation therefore depends on competition between the rate of decay of the electronic resonance state and the timescale of induced motion the molecule experiences in the excited potential energy surface. Provided large equilibrium displacements between the neutral and resonant state surfaces, the resulting dynamics can lead to substantial excitation of molecular motion.

While the lifetime and equilibrium displacement of the resonance state are, in principle, unrelated, the nature of the chemical systems involved implies that in practice a correlation between the two attributes is generally expected. In systems where the electrode–molecule coupling is weak, the lifetimes are long and the electronic orbitals are typically spatially localized. In such systems one expects rearrangement of the molecular backbone in the course of the transient charging event, translating into large equilibrium displacement of the resonance with respect to the initial state and consequently a substantial probability for energy transfer to the molecule. At the opposite extreme, where the coupling of the molecular moiety to the electrodes is strong, the resonance lifetime is expected to be small and the electronic orbitals are generally delocalized across the system, giving rise to small equilibria displacements. In such instances, we expect current-driven dynamics to be minimal. These qualitative arguments suggest that a correlation between the interface interaction and the observed dynamics can be identified based on the degree of charge localization in the junction.

In what follows we provide a direct study of the effect of charge localization in a simple model system, which exemplifies the basic principles of current-induced dynamics and, in addition, offers rich quantum effects and interesting potential. Specifically, we examine a molecular rattle, consisting of a $Li^+C_9H_9^-$ zwitterion[47] contacted to two Al reservoirs. We begin in the second section by making use of ab initio electronic structure calculations to construct potential energy curves for a series of systems with varying degrees of charge localization on a molecular moiety. The resulting wave packet dynamics are presented and their quantum nature is explored in the third section. In the final section we discuss the connection between the degree of localization of the electronic orbitals in energy and coordinate spaces, the contact interaction, and the current-driven dynamics.

ELECTRONIC STRUCTURE

We consider the model system shown in Fig. 1, which consists of a lithium ion attached to a nine-member carbon ring ion placed between two Al clusters. This model system was selected based on the anticipation of interesting dynamics for the lithium atom as it is driven by the current to tunnel from one side of the carbon ring to the other. In order to investigate the charge localization effects in this junction, we systematically vary the size of the metal clusters to develop a series of models wherein the electronic orbitals are increasingly delocalized. In each case, the initial structure is optimized and single point energies are calculated for the neutral and negatively charged states while varying the vertical distance of the lithium atom from the center of the carbon ring. We use Density Functional Theory (DFT) with a LANL2DZ basis set[48] and the B3LYP exchange-correlation functional.[57] The calculations were done using Q-CHEM V2.0.[50]

The resulting potential curves for the four different cluster sizes are shown in Fig. 2. The presence of a gate voltage is taken into account by adding a linear potential perpendicular to the ring plane as indicated by triangles in Fig. 2. For symmetric molecule+clusters junctions, one expects a symmetric double-well potential energy curve, where the two minima correspond to the equilibrium position of the Li above and below the plane of the carbon ring, and the barrier corresponds to the symmetric configuration, where the Li atom is in the center of the ring. Such symmetric junctions are obtained through energy minimization in the cases of one, three, and four atom clusters, and the corresponding symmetric double-

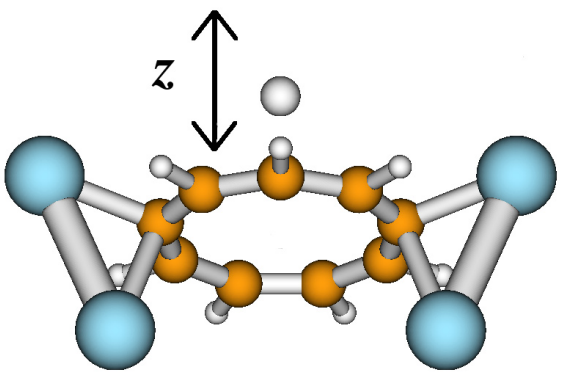

Fig. 1. Illustration of the model system considered, which consists of a $Li^+C_9H_9^-$ zwitterion attached between two Al clusters of varying size. Inelastic resonant current gives rise to a rattle motion, where the Li is threaded back and forth through the carbon ring. For 1-Al, 3-Al, and 4-Al atom clusters the equilibrium configuration is symmetric, whereas for 2-Al clusters it is asymmetric.

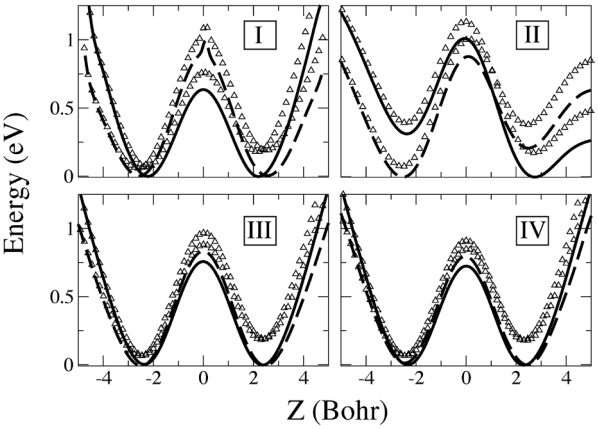

Fig. 2. Potential energy curves for motion of the lithium atom along the axis perpendicular to the plane of the carbon ring (See Fig. 1) for the neutral (solid curve) and ionic (dashed curve) states. The size of the cluster corresponding to each set of curves is indicated by roman numerals. The curves consisting of small triangles denote the molecular potentials with the application of a 0.25 V gate potential.

well curves are shown in Fig. 2(I), (III), and (IV). In the neutral state, the barrier to tunneling between the two minima is ca. 0.7 eV, and the Li ion is localized above and below the plane with vanishingly small tunneling probability. In the charged state, the excess electron localizes partially on the carbon ring, causing an additional repulsion between the atom and the ring and hence larger equilibrium distances of the lithium atom from the ring plane. It is the equilibrium displacement of the resonant, with respect to the initial, state that leads to large amplitude vibration of the Li–ring coordinate in the neutral state subsequent to electronic relaxation of the transient ionic state. This vibrational excitation results in facile tunneling between the two wells, as discussed in the next section. It should be noted that when dealing with small clusters of only a few aluminum atoms, the minimum energy configuration is not necessarily symmetric. For the present model, in the case of the two-atom clusters, the minimum energy configuration is asymmetric, resulting in asymmetric potential energy curves, as shown in Fig. 2(II). These effects are not anticipated in larger cluster systems and in fact are not observed in the other systems studied here.

Inspection of Fig. 2 shows several trends that agree with our intuition. In examining the one- and two-atom clusters, we find that the charged and neutral state curves differ by a greater amount than in the case of the three- and four-aluminum clusters. For the smaller aluminum clusters, the minima of the wells are displaced by greater amounts in the ionic state and the tunneling barriers increase to a greater extent. These observations suggest that the excess electron is largely localized on the carbon ring, giving rise to the greater repulsion. In the instances of the larger clusters, the potential energy curves are seen to approach asymptotic forms with respect to cluster size. The displacements are a factor of four smaller in the ionic state and the barrier height increase is similarly about a factor of four less than in the case of one aluminum atom. In these instances, the repulsion of the excess electron has a lesser effect on the lithium since it is more delocalized across the entire molecule plus clusters junction. For the system at hand, the limit of a delocalized state, with resultant vanishingly small equilibrium displacement, is attained quickly, with as small an electrode as a four-atom cluster.

DYNAMICS

The current-driven dynamics in a general quantum junction can be computed within the scattering theory of refs 26, 24, where an open system nonequilibrium solution of the electronic dynamics is combined with a realistic solution of the time-dependent Schrödinger equation for the nuclear subspace, taking into proper account the coordinate-dependence of the electronic relaxation rate. Here, however, our interest is in exploring general trends, rather than in providing an accurate description of a specific junction. We therefore adopt the simplest model that is capable of extracting the essential physics. As such, we consider the model of Menzel and Gomer[52] and Redhead[53] (MGR), which has been widely applied to the description of substrate-mediated photochemistry.[51] Within this model, observables are computed through a lifetime-averaging procedure that neglects the coherence effects and assumes that the electronic relaxation is independent of coordinates. Thus, the initial wave function (a vibrational eigenstate of the neutral state Hamiltonian or a thermal average thereof) is instantaneously promoted to the charged state potential energy surface, allowed to evolve for a time τ_R, and then instantaneously returned to the neutral state surface. Once results have been collected over a sufficiently large range of τ_R values, $0 \leq \tau_R \leq \tau_R^m, \tau_R^m \gg \tau$, where τ is the resonance lifetime, the τ_R-dependent observables $O(\tau_R)$ are incoherently averaged over τ_R to yield the observable of interest $O(\tau) = \tau^{-1} \int d\tau_R \exp(-\tau_R/\tau) O(\tau_R)$. A second average over the Boltzmann distribution of the initial vibrational levels of the lithium atom is performed if the parent state is a thermal average. In the present study the initial states are generated by direct diagonalization of the ground state Hamiltonian, written within a discrete variable representation,[55] and the wave packet propagation on the two coupled states is carried out using the split operator technique.[54] The observable of interest here is the

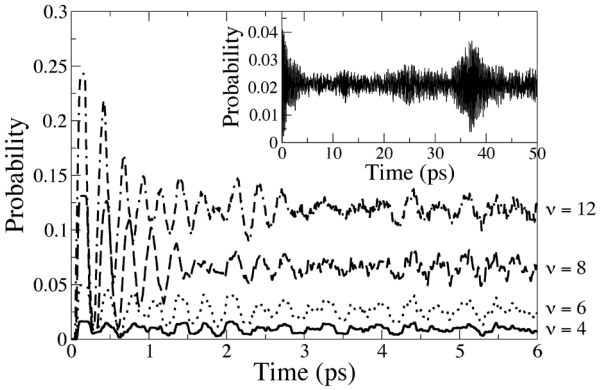

Fig. 3. The probability density in the raised well of the double-well potential as a function of time for one-atom clusters, where the initial vibrational level is $\upsilon = 4$ (solid), $\upsilon = 6$ (dotted), $\upsilon = 8$ (dashed), and $\upsilon = 12$ (dot–dashed). The results for $\upsilon = 4$ have been scaled by a factor of 6. The inset shows the long time revival dynamics of the vibrational wave packet for an initial vibrational state $\upsilon = 10$.

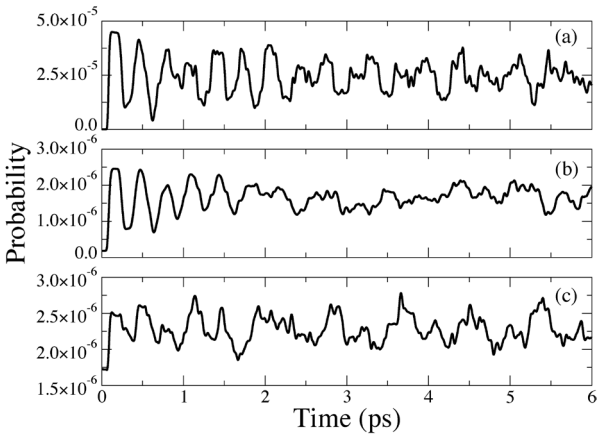

Fig. 4. Boltzmann averaged probability densities in the raised well of the double-well potential vs. time at a temperature 600 K. (a) One-atom clusters, (b) three-atom clusters, and (c) four-atom clusters.

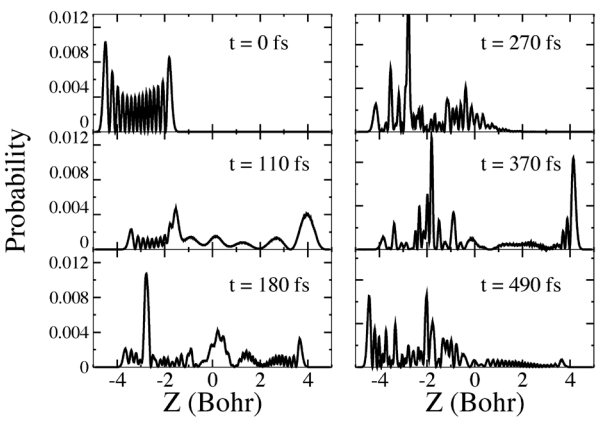

Fig. 5. Time evolution of the probability density associated with vibrational wave function $\upsilon = 14$ after propagating on the ionic potential for $\tau_R = 60$ fs.

probability of finding the system in the raised well of the double-well model as a function of time subsequent to the resonance electron scattering event.

The above scheme was applied to the four sets of potentials shown as solid curves in Fig. 2, corresponding to the four junctions of Fig. 1. In order to focus on the effect of charge localization in physical space, artificially disentangled from the effect of the resonance lifetime, we fix the latter parameter at a representative value of 60 fs in all calculations. In realistic junctions, this parameter depends sensitively on the interface interaction and its effects are thus entangled to a certain extent with those of charge localization. Often it varies over 1–2 orders of magnitude within a single junction.[37]

The results of the dynamical simulations for the one-, three-, and four-atom cluster junctions are shown in Figs. 3 and 4. While calculations were also performed for the two-atom cluster junction, it is clear that the initial vibrational level required to observe appreciable interwell tunneling in this junction is much larger than the range of vibrational levels that are thermally accessible at the temperatures considered. We first remark, Fig. 4, that the interwell tunneling probability is orders of magnitude lower for the three- and four-atom cluster junctions than for the one-atom cluster case. This result illustrates the sensitivity of the mechanism to the differences between the neutral and charged state surfaces and hence to the charge localization. A reduction in the equilibrium displacements by a factor of four has the effect of damping the interwell tunneling by orders of magnitude.

The dynamics for the one-Al atom cluster junction, corresponding to spatially-localized electronic orbitals, are of greater interest and more transparently capture the quantum nature of the double-well problem. In order to understand the thermally averaged probabilities of Fig. 4a, we first consider the initial-state-resolved results for vibrational levels $\upsilon = 0$ to $\upsilon = 15$, a selection of which is illustrated in Fig. 3. For each of the parent vibrational levels considered, the probability begins to build up in the raised well of the double-well potential within ca. 50 fs and remains constant for several tens of femtoseconds. The initial build up of probability density can be attributed to the motion of a high energy portion of the wave packet upon relaxation to the neutral surface. The resonant electron scattering event transfers sufficient energy from electronic into vibrational degrees of freedom for a portion of the thus populated wave packet to penetrate the interwell barrier. As evidenced by the evolution of the wave packet in Fig. 5, this portion of the wave packet traverses the barrier region and subsequently shuttles between the two wells on a timescale of ca. 250 fs, exhibiting quasi-periodic motion. The

strong anharmonicity of the potential gives rise to rapid dephasing, on a timescale of 8–10 periods. Since coherence (within the complete electronic vibrational space) is maintained in the present model, the wave packet undergoes a characteristic revival phenomenon, where the initial motion is reconstructed, subsequent to which the periodic interwell shuttling is reinstated.

The trends in our simulations for the lithium threading through the carbon ring fit the general conjecture presented at the outset of this work with regard to the effects of charge localization. When we allow for a greater degree of charge localization on the molecular moiety of the junction, we find amplified dynamics. This extreme corresponds readily to the case of weak coupling of the molecule to the electrodes and is expected, e.g., in the fullerene-bases junctions of refs 1 and 56 and to certain STM experiments.[14,32,33] Here large equilibrium displacements allow for greater inelasticity of the resonant current, leading to events such as desorption and reaction. As the size of the aluminum clusters increases, charge delocalization is enhanced and the dynamics are suppressed. The connection here is with the case of strongly coupled junctions, the familiar examples of which are organic molecules attached to gold electrodes via a sulfur group.

CONCLUSIONS

One goal of the study discussed in the previous sections was to gain an understanding of the role of charge localization in resonance scattering through molecular junctions. We found that localization has a substantial impact on scattering dynamics and provides a general guideline for anticipating dynamical events in the device environment. Our study focused on a simple model of a $Li^+C_9H_9^-$ molecule attached to two aluminum clusters. By varying the size of the aluminum clusters we systematically varied the degree of delocalization of the orbitals that dominate the current, and hence the extent of inelasticity.

More generally, one expects the degree of delocalization in molecular junctions to be controllable through choice of the contact groups that link the molecular moiety to the electrodes, as well as by choice of the substrate. Thus, the classic choice of a sulfur atom to link an organic molecule to gold electrodes optimizes the charge delocalization and results in good conductivity and at most minor current-driven dynamics. Substitution of the S-atom by an N-atom, for instance, would give rise to enhanced dynamics. Likewise, we expect silicon-based molecular junctions to offer enhanced charge localization and opportunities for current-driven dynamics as compared to the conventional metal-base molecular electronics. While construction of the junction to enhance charge localization is desired for applications such as current-driven molecular machines, its construction to enhance charge delocalization is desired for the development of stable junctions with good conductance.

Our model system deliberately (and artificially) focused on the role of charge localization alone. In realistic junctions modification of the linking groups or the substrate changes also the resonance lifetime. The latter parameter has a more complex effect, since a longer lifetime increases the probability of current-driven dynamics per resonant event but decreases the probability of excitation of the resonance (that is, the resonant portion of the current).

A second goal of this study has been to explore the $Li^+C_9H_9^-$ zwitterion as a potential molecular rattle, a prototype for a current-triggered molecular machine with the general advantage of being individually-driven in the dry state. By contrast to the current-driven molecular machines explored in previous work,[37–39] where the nuclear motion could be understood classically, the rattle exhibits purely quantum effects in the nuclear subspace. In particular, tunneling through the barrier corresponding to the planar configuration is triggered by the resonance inelastic electron tunneling event, resulting in coherent wave packet oscillations at a period corresponding to the barrier crossing time. Substantial anharmonicity gives rise to rapid wave packet dephasing, on the timescale of ca. 10 cycles, with revivals occurring on a ca. 10 times longer timescale. Whereas the short time threading of the Li atom through the ring, corresponding to the early wave packet vibrations, is expected also in the molecular junction analog with sufficient charge localization, the long time coherent motion is clearly a feature of the small cluster model, and would be damped due to vibrational relaxation in more extended systems.

Acknowledgments. The authors are grateful to the National Science Foundation (Grant No. DMR-0520513) and to the US-Israel Binational Science Foundation for support.

REFERENCES AND NOTES

(1) Park, H.; Park, J.; Lim, A.K.L.; Anderson, E.H.; Alivisatos, A.P.; McEuen, P.L. *Nature* **2000**, *407*, 57–60.
(2) Park, H.; Lim, A.K.L.; Alivisatos, A.P.; Park, J.; McEuen, P.L. *Appl. Phys. Lett.* **1999**, *75*, 301–303.
(3) Park, J.; Pasupathy, A.N.; Goldsmith, J.I.; Chang, C.; Yaish, Y.; Petta, J.R.; Rinkoski, M.; Sethna, J.P.; Abruna, H.D.; McEuen, P.L.; Ralph, D.C. *Nature* **2002**, *417*, 722–725.
(4) Liang, W.J.; Shores, M.P.; Bockrath, M.; Long, J.R.; Park, H. *Nature* **2002**, *417*, 725–729.

(5) Reed, M.A.; Zhou, C.; Miller, C.J.; Burgin, T.P.; Tour, J.M. *Science* **2000**, *278*, 252–254.
(6) Smit, R.H.M.; Noat, Y.; Untiedt, C.; Lang, N.D.; van Hemert, M.C.; van Ruitenbeek, J.M. *Nature* **2002**, *419*, 906–909.
(7) Reichert, J.; Ochs, R.; Beckmann, D.; Weber, H.B.; Mayor, M.; Löhneysen, H.v. *Phys. Rev. Lett.* **2002**, *88*, 176804.
(8) Kergueris, C.; Bourgoin, J.-P.; Palacin, S.; Esteve, D.; Urbina, C.; Magoga, M.; Joachim, C. *Phys. Rev. B* **1999**, *59*, 12505–12513.
(9) Joachim, C.; Gimzewski, J.K. *Europhys. Lett.* **1995**, *30*, 409–414.
(10) Rawlett, A.M.; Hopson, T.J.; Nagahara, L.A.; Tsui, R.K.; Ramachandran, G.K.; Lindsay, S.M.; Joachim, C.; Gimzewski, J.K. *Appl. Phys. Lett.* **2002**, *81*, 3043–3045.
(11) Bumm, L.A.; Arnold, J.J.; Cygan, M.T.; Dunbar, T.D.; Burgin, T.P.; Jones II, L.; Allara, D.L.; Tour, J.M.; Weiss, P.S. *Science* **1996**, *271*, 1705–1707.
(12) Cui, X.D.; Primak, A.; Zarate, X.; Tomfohr, J.; Sankey, O.F.; Moore, A.L.; Moore, T.A.; Gust, D.; Nagahara, L.A.; Lindsay, S.M. *J. Phys. Chem. B* **2002**, *106*, 8609–8614.
(13) Xu, B.; Tao, N.J. *Science* **2003**, *301*, 1221–1223.
(14) Guisinger, N.P.; Yoder, N.L.; Hersam, M.C. *Proc. Natl. Acad. Sci. USA* **2005**, *102*, 8838–8843.
(15) Xue,Y.; Ratner, M.A. *Phys. Rev. B* **2004**, *69*, 85403.
(16) Luo, Y.; Wang, C.-K.; Fu, Y.J. *Chem. Phys.* **2002**, *117*, 10283–10290.
(17) Ke, S.-H.; Baranger, H.U.; Yang, W. *J. Am. Chem.* Soc. **2004**, *126*, 15897–15904.
(18) Basch, H.; Ratner, M.A. *J. Chem. Phys.* **2003**, *119*, 11926–11942.
(19) Basch, H.; Cohen, R.; Ratner, M.A. *Nano Lett.* **2005**, *5*, 1668–1675.
(20) Taylor, J.; Brandbyge, M.; Stokbro, K. *Phys. Rev. Lett.* **2002**, *89*, 138301.
(21) Di Ventra, M.; Pantelides, S.T.; Lang, N.D. *Phys. Rev. Lett.* **2000**, *84*, 979–982.
(22) Emberly, E.G. ; Kirczenow, G. *Phys. Rev. B* **1998**, *58*, 10911–1920.
(23) Magoga, M.; Joachim, C. *Phys. Rev. B* **1997**, *56*, 4722–4729.
(24) Yaliraki, S.N.; Kemp, M.; Ratner, M.A. *J. Am. Chem. Soc.* **1999**, *121*, 3428–3434.
(25) Xue, Y.; Ratner, M.A. *Phys. Rev. B* **2003**, *68*, 115407.
(26) Seideman, T. *J. Phys.: Condens. Matter* **2003**, *15*, R521–R549.
(27) Mayne, A.J.; Dujardin, G.; Comtet, G.; Riedel, D. *Chem. Rev.* **2006**, *106*, 4355–4378.
(28) Saalfrank, P.; Nest, M.; Andrianov, I.; Klamroth, T.; Kröner, D.; Beyvers, S. *J. Phys.: Condens. Matter* **2006**, *18*, S1425–S1459.
(29) Ueba, H. *Surf. Rev. Lett.* **2003**, *10*, 771–796.
(30) Ho, W.J. *Chem. Phys.* **2002**, *117*, 11033–11061.
(31) Hod, O.; Baer, R.; Rabani, E. *Phys. Rev. Lett.* **2006**, *97* (26), 266803.
(32) Yoder, N.L.; Guisinger, N.P.; Hersam, M.C.; Jorn, R.; Kaun, C.-C.; Seideman, T. *Phys. Rev. Lett.* **2006**, *97*, 187601.
(33) Alavi, S.; Rousseau, R.; Patitsas, S.N.; Lopinski, G.P.; Wolkow, R.A.; Seideman, T. *Phys. Rev. Lett.* **2000**, *85*, 5372–5375.
(34) Foley, E.T.; Kam, A.F.; Lyding, J.W.; Avouris, P. *Phys. Rev. Lett.* **1998**, *80*, 1336–1339.
(35) Pascual, J.I.; Lorente, N.; Song, Z.; Conrad, H.; Rust, H.-P. *Nature* **2003**, *423*, 525–528.
(36) Lastapis, M.; Martin, M.; Riedel, D.; Hellner, L.; Comtet, G.; Dujardin, G. *Science* **2005**, *308*, 1000–1003.
(37) Kaun, C.-C.; Seideman, T. *Phys. Rev. Lett.* **2005**, *94*, 226801.
(38) Kaun, C.-C.; Jorn, R.; Seideman, T. *Phys. Rev. B* **2006**, *74*, 45415.
(39) Kral, P.; Seideman, T. *J. Chem. Phys.* **2005**, *123*, 184702.
(40) Jorn, R.; Seideman, T. *J. Chem. Phys.* **2006**, *124*, 84703.
(41) Ueba, H.; Mii, T.; Lorente, N.; Persson, B.N.J. *J. Chem. Phys.* **2005**, *123*, 84707.
(42) Liu, K.; Gao, S. *Phys. Rev. Lett.* **2005**, *95*, 226102.
(43) Abe, A.; Yamashita, K.; Saalfrank, P. *Phys. Rev. B* **2003**, *67*, 235411.
(44) Teillet-Billy, D.; Gauyacq, J.P.; Persson, M. *Phys. Rev. B* **2000**, *62*, R13306–R13309.
(45) Gadzuk, J.W. *Phys. Rev. B* **1991**, *44*, 13466–13477.
(46) Gao, S.; Persson, M.; Lundquist, B.I. *Phys. Rev. B* **1997**, *55*, 4825–4836.
(47) Das, B.; Sebastian, K.L. *Chem. Phys. Lett.* **2002**, *365*, 320–326.
(48) Hay, P.J.; Willard, R.W. *J. Chem. Phys.* **1985**, *82*, 299.
(49) Becke, A.D. *J. Chem. Phys.* **1993**, *98*, 1372.
(50) Kong, J.; White, C.A.; Krylov, A.I.; et al. *J. Comput. Chem.* **2000**, *21* (16), 1532.
(51) Guo, H.; Saalfrank, P.; Seideman, T. *Prog. Surf. Sci.* **1999**, *62*, 239–303.
(52) Menzel, D.; Gomer, R. *J. Chem. Phys.* **1964**, *41*, 3311–3328.
(53) Redhead, P. *Can. J. Phys.* **1964**, *42*, 886–905.
(54) Fleck, J.; Morris, J.; Feit, M. *Appl. Phys.* **1976**, *10*, 129.
(55) Colbert, D.T.; Miller, W.H. *J. Chem. Phys.* **1992**, *96*, 1982–1991.
(56) Pasupathy, A.N.; Park, J.; Chang, C.; Soldatov, A.V.; Lebedkin, S.; Bialczak, R.C.; Grose, J.E.; Donev, L.A.K.; Sethna, J.P.; Ralph, D.C.; McEuen, P.L. *Nano Lett.* **2005**, *5*, 203–207.
(57) (a) Becke, A.D. *J. Chem. Phys.* **1993**, *98*, 5648. Lee, T.J.; York, D.M.; Yang, W. *J. Chem. Phys.* **1996**, *105*, 2744.